On the implementations of Circuit Models of Arcs

Simon Le Blond, Brian Ross, and Vančo Litovski

Abstract - Fault arc models are increasingly important for design of modern power system protection algorithms. Several solutions were reported in the literature but no comparisons of the behaviour were given. Furthermore, in fact, while all models are based on solving a differential equation where the conductance of the arc is unknown, not much of the conductance was reported the main concerns being oriented towards the voltage, current and power of the arc. This paper thus initially presents electrical circuits that implement existing arc model equations. Namely, a circuit in which one node voltage equals the arc conductance is developed for every model. These then were simulated and the resulting arc conductances are reported and compared here.

Keywords - arcing, arc modelling, arc simulation, circuit model
.

1. INTRODUCTION

Arcing faults in power systems can cause considerable damage, even explosions, despite the installed protection system [1] [2]. In fact numerous failures occurring in these systems may be attributed to arcing which in its initial stage leads to fault currents between two conductors. Depending on the parameters of the electrical network, such as power source and equivalent impedance, these failures may lead to stable arcs provided both the protection system fails to activate and no self-extinguishing process is started. After arc extinction and reenergizing the system, the phenomenon can reappear, depending on the level of the driving voltage and the load current, and also depending on the performance of the partly damaged insulation, characterized by its thickness and chemical composition.

Thus the diagnosis and location of such a fault when it occurs or, even better, correct prediction before it fully develops, is of prime importance for proper maintenance and protection of the power distribution system. Crucial to the development of any diagnostic and fault prediction system is a simulator that supplements difficult, disruptive, and expensive experiments on real LV power systems. Vital to the simulator, in turn, are models that capture the properties of the specific components of the system and when instantiated behave as faithfully as the real components as possible. Such models must be accurate, so one may depend on the simulation results; must be robust, putting no limits to realistic signal's amplitudes and waveforms; must be simple, enabling fast simulation of complex systems to which the modelled device belongs; and be easy to represent

Simon Le Blond, Brian Ross, and Vančo Litovski are with the University of Bath, Uk, {sp.leblond; bp.ross; v.litovski}@bath.ac.uk

in software in a form convenient for frequent instantiation.

One may now categorize the existing models, already mentioned in the Introduction, into the following groups:

1. The high impedance model (HI), described by an equation of the form

(1) $G(t)=f(G_0,\tau,t);$

2. The models describing electro-thermal dynamics of the arc described by an equation of the form

(2) $\dfrac{1}{G(t)}\cdot\dfrac{dG(t)}{dt} = f(G_0,\tau,\mathbf{c},i(t),v(t),P(t))\,,$

$\mathbf{c}$ being a set of constants;

3. The non-equilibrium models described by an equation of the form

(3) $\dfrac{1}{G(t)}\cdot\dfrac{dG(t)}{dt} = f\left(G_0,\tau,\mathbf{c},i(t),v(t),P(t),\dfrac{dv(t)}{dt}\right),$

and

4. The model involving ablation described by an equation of the form

(4) $\dfrac{1}{G(t)}\cdot\dfrac{dG(t)}{dt} = f\big(G_0,\tau,\mathbf{c},i(t),v(t),P(t),L(t),S(t)\big).$

The following notation was used: t for the time variable, G for the arc conductance, G_0 for its initial value, $i(t)$ for the arc current, $v(t)$ for the arc voltage, $P(t)$ for the arc power, $L(t)$ for the arc length, and $S(t)$ for the arc area.

From electrical modelling and simulation point of view there is a fundamental difference between the first one and the last three. Namely, if the HI model is to be implemented the arc conductance will start with zero (open circuit) and will rise to a prescribed value (G_0) no matter what happens with the currents and voltages. In the rest of the cases the conductance stars with some initial value (which may be high) and, depending on the model and the model parameters, rises or decreases in time.

The existing models as given in the literature [3] [4] [5] [6] were first studied from the applicability in a circuit form. Having in mind that (3) in fact represents one differential equation containing time derivatives of two different variables we first excluded (3) as candidate for circuit modelling. Then, we supposed that the arc length and the arc area are constant reducing (4) into (2). Therefore, (1) and (2) were left and used for further study.

Electrical circuits convenient for implementation in circuit simulators recognizing behavioural descriptions were developed for every single arc model found in the literature. These were then simulated while excited by a sinusoidal voltage source of amplitude of 380 V and of power frequency of 50 Hz having internal resistance of 1 mΩ. As a simulation results the solutions of (1) or (2) were taken and demonstrated here. To make the comparison adequate equal or similar parameter values were used for different model in the largest possible extent.

Since, to our best knowledge, no reports of this kind were published we consider the results depicted below as an asset to build on, so no special comments on the appropriateness of any of them were given.

The analysis will follow the order already established in the literature such as [4] [5]. To get feeling as to what are the differences between the models and to save space simulation results will be given on one figure only.

It is important to note that these models were developed with an intention to simulate arcs in the open (including air, vacuum, and oil as an environment). That means they are supposed to be fed by a source of very low resistance. To allow for that, in the simulations reported here, internal resistance of the proper voltage source of 1 mΩ was used.

The paper is structured so that the models are visited in succession and circuits are proposed for each one of them. Then simulation results are given collectively.

2. CREATION OF THE ARC MODEL AND SIMULATION RESULTS

In this section a review of the existing models will be given. For every one of them a circuit will be proposed that enables implementation of the model within a circuit simulator.

2.1 The high impedance model (HI)

A time varying conductance reported in [6] and implemented also in [7] [8] [9] may be used to model the arc occurring between two power lines or between a line and ground. Namely, it is proposed that the arc conductance is obeying the following differential equation

$$(1) \qquad \frac{\mathrm{d}G(t)}{\mathrm{d}t} = \frac{1}{\tau}(G_0 - G(t))$$

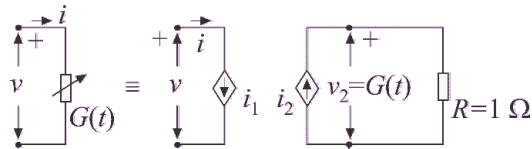where G_0 and τ are model parameters.

Figure 1. Resistive circuit modelling the nonlinear conductance given by (2)

The solution of this equation is

$$(2) \qquad G(t) = G_0(1 - e^{-t/\tau}).$$

As can be seen, in this case, the value of the arc conductance at the beginning of arcing is zero, meaning infinite resistance, and ends up at the end of the arcing process with the value G_0 which is a model parameter usually obtained by measurement. τ is the other parameter which may here be interpreted as the time constant of the arcing and, again, obtained by measurement.

This conductance may be modelled by the circuit of Fig. 2 where

$$(3) \qquad i_1 = v \cdot v_2$$

$$(4) \qquad i_2 = G_0(1 - e^{-t/\tau}).$$

We assume that the arcing starts not at the very beginning of the simulation which means that the time variable in (1) is not the real time but a new variable shifted to the arcing instant. To create a time variable that starts with zero at t_0 and ends with $\Delta t = t_1 - t_0$ at t_1 the circuit of Fig. 2 may be used.
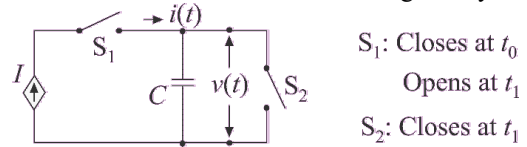
Figure 2. A circuit generating a voltage proportional to time. $t_1 > t_0$.

For this circuit one may state that

$$(5) \qquad v(t) = \begin{cases} 0 & \text{for } t < t_0 \\ \dfrac{I}{C}(t - t_0) & \text{for } t_0 < t < t_1 \\ 0 & \text{for } t > t_1 \end{cases}.$$

Here t_0 is the time instant when the fault occurs while $\Delta t = t_1 - t_0$ is the duration of the fault. One may say that a protective device was activated (or some other remedial action was undertaken) at t_1. In that way, if we substitute t by $v(t)$ in (4), we will have a time dependent conductance that starts changing at t_0 and falls back to zero at t_1.

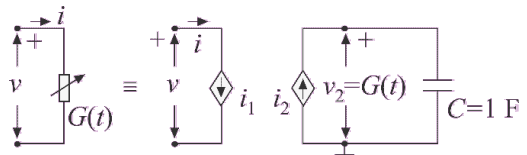In the subsequent simulation experiments t_0=50 ms, t_1=150 ms and C=1 F were used.

Figure 3. Electrical circuit generating the solution of the differential equation governing the arcing process

In order to unify the simulation, however, instead of using

the closed form expression for the conductance given by (2) we will use a circuit that solves the differential equation (1) during the simulation. To that end the circuit of Fig. 3 was used. In this case we have

(6a) $\quad i_1 = v \cdot v_2$

(6b) $\quad i_2 = \dfrac{1}{\tau}(G_0 - G(t)) \cdot$

To implement the model for verification and testing purposes we used the circuit depicted in Fig. 4. It consists of a sinusoidal source with internal resistance R_0, and a switch that activates the arc at $t=t_0$ and deactivates it at $t=t_1$.
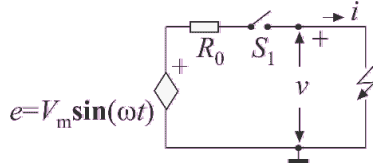

Figure 4. The simple circuit used for verification and characterization of the model

The simulation results for this type of arc model are depicted in Fig. 5 (denoted by 1). $G_0=100$ S and $\tau=0.04$ s were used.

2.2 The Cassie model

This model was first published in [10]. It is expressed in the following form:

(7) $\quad \dfrac{1}{G(t)} \cdot \dfrac{dG(t)}{dt} = \dfrac{1}{\tau}\left(\dfrac{v^2}{V_c^2} - 1\right).$

Note that since, at $v(0)=0$,

(8) $\quad \dfrac{1}{G(0)} \cdot \dfrac{dG(t)}{dt}\bigg|_{t=0} = -\dfrac{1}{\tau},$

$G(0)$ determines the initial value of the conductance (which is not specified by the model as such), while $-G(0)/\tau$ represents its slope at the origin. Accordingly, the model is defined by three parameters: τ, V_c, and $G(0)$.

With reference to Fig. 3, in this case we have

(9a) $\quad i_1 = v \cdot v_2$

(9b) $\quad i_2 = -\dfrac{1}{\tau} \cdot v_2 + \dfrac{1}{\tau \cdot V_c^2} \cdot v_2 \cdot v^2.$

The value of $G(t)$ corresponding to the one expressed by (7), obtained by running the circuit of Fig. 4 by SPICE, is depicted in Fig. 5 denoted by 2. The following parameters were used for this simulation: $R_0=1$ mΩ, $G_0=100$ S, $\tau=10$ ms, and $V_C^2 = 1000$ V.
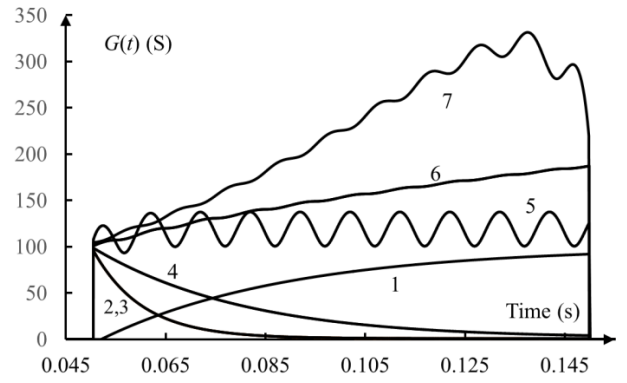

Figure 5. Conductance $G(t)$ for various models
1. High impedance model
2. Cassie model
3. Schewemacher model
4. Schwarz model
5. Mayr model
6. Modified Mayr model
7. Habedank model

It is important to note that Equ. (9) has a solution

(10) $\quad G(t)=G(0)\cdot e^{-t/\tau}$

even in the absence of any voltage at the arc terminals. That means that exponential decay of the arc conductance is expected since, after breakdown, one may expect $v(t)<V_c$ or even $v(t)<<V_c$ and (10) is practically governing the process.

It also means that, in the case of a short duration of the arc, the time of activation of the arc should be set to zero at the activation moment and, after the arc is extinguished, the capacitor (In Fig. 3) should be short-circuited to discharge.

2.3 The Schwarz arc model

The Schwarz arc model [11] may be expressed as:

(11) $\quad \dfrac{1}{G(t)} \cdot \dfrac{dG(t)}{dt} = \dfrac{1}{\tau \cdot G^a(t)}\left(\dfrac{v \cdot i}{P \cdot G^b(t)} - 1\right).$

where P is the cooling constant, while a and b are constants. It is a four parameter model which may be stated as a black-box since the parameters a and b have no physical interpretation. a and b are in fact fitting parameters.

For circuit simulation it will be expressed schematically on the same way as the Cassie circuit i.e. by Fig. 3, while the corresponding current sources will be expressed in the following way

(12a) $\quad i_1 = v \cdot v_2$

(12b) $\quad i_2 = -\dfrac{1}{\tau} \cdot v_2^{1-a} + \dfrac{1}{\tau \cdot P} \cdot v_2^{1-a-b} \cdot v \cdot i$

The value of $G(t)$ corresponding to the one expressed by (11), obtained by running the circuit of Fig. 4 by SPICE, is

depicted in Fig. 5 denoted by 4. The following parameters were used for this simulation: $R_0=1$ mΩ, $G_0=100$ S, $\tau=100$ ms, and $P=1$ W, $a=0.1$ and $b=0.15$.

2.4 Model Mayr model and modified Mayr

This model was frequently implemented [11] [12] [13] [4].

The original Mayr equation is as follows:

$$(13) \quad \frac{1}{G(t)} \cdot \frac{dG(t)}{dt} = \frac{1}{\tau}\left(\frac{v^2(t)G(t)}{P_0} - 1\right).$$

Using the circuit of Fig. 3 one may express the model as

$$(14a) \quad i_1 = v \cdot v_2$$

$$(14b) \quad i_2 = -\frac{1}{\tau} \cdot v_2 + \frac{1}{\tau \cdot P_0} \cdot v_2^2 \cdot v^2.$$

The value of $G(t)$ corresponding to the one expressed by (13), obtained by running the circuit of Fig. 4 by SPICE, is depicted in Fig. 5 denoted by 4. The following parameters were used for this simulation: $R_0=1$ mΩ, $G_0=100$ S, $\tau=10$ ms, and $P=100$ W.

The modified Mayr model [14] is described by the following equation

$$(15) \quad \frac{1}{G(t)} \cdot \frac{dG(t)}{dt} = \frac{1}{\tau}\left(\frac{v(t) \cdot i(t)}{P_0 + C \cdot |i|} - 1\right).$$

The corresponding controlled sources of Fig. 3, now are

$$(16a) \quad i_1 = v \cdot v_2$$

$$(16b) \quad i_2 = -\frac{1}{\tau} \cdot v_2 + \frac{1}{\tau} \cdot v \cdot i \cdot \frac{v_2}{P_0 + C \cdot \sqrt{i^2}}.$$

The value of $G(t)$ corresponding to the one expressed by (15), obtained by running the circuit of Fig. 4 by SPICE, is depicted in Fig. 5 denoted by 6. The following parameters were used for this simulation: $R_0=1$ mΩ, $G_0=100$ S, $\tau=10$ ms, $C=50$ V, and $P=1000$ W.

2.5 The Habedank Model

The model equations proposed by Habedank [15] are

$$(17a) \quad \frac{1}{G_c(t)} \cdot \frac{dG_c(t)}{dt} = \frac{1}{\tau_c}\left(\frac{v^2(t)G^2(t)}{V_c^2 G_c^2(t)} - 1\right)$$

$$(17b) \quad \frac{1}{G_m(t)} \cdot \frac{dG_m(t)}{dt} = \frac{1}{\tau_m}\left(\frac{v^2(t)G^2(t)}{P_0 G_m(t)} - 1\right)$$

$$(17c) \quad \frac{1}{G(t)} = \frac{1}{G_c(t)} + \frac{1}{G_m(t)}$$

where $G_c(t)$ is the arc conductance in the Cassie equation, τ_c

is the Cassie time constant, $G_m(t)$ is the arc conductance in the Mayr equation, τ_m is the Mayr time constant and P_0 is a constant. In fact here one has *two nonlinear time dependent mutually coupled conductances in a system with six free parameters*: τ_c, V_c, $G_c(0)$ and τ_m, V_m, $G_m(0)$. That is a serious challenge from the parameter extraction and implementation point of view since positive feedback may be set for some combination of the parameters.

To get the circuit representation of this series connection we will first substitute resistances in place of the conductances. In that way the Habedank model will be expressed as

$$(18a) \quad -\frac{1}{R_c(t)} \cdot \frac{dR_c(t)}{dt} = \frac{1}{\tau_c}\left(\frac{v^2(t) \cdot [R_c(t)+R_m(t)]^2}{V_c^2 \cdot R_m^2(t)} - 1\right)$$

$$(18b) \quad -\frac{1}{R_m(t)} \cdot \frac{dR_m(t)}{dt} = \frac{1}{\tau_m}\left(\frac{v^2(t) \cdot [R_c(t)+R_m(t)]^2}{P_0 \cdot R_m(t) \cdot R_c^2(t)} - 1\right)$$

$$(18c) \quad R(t)=R_c(t)+R_m(t).$$

For a given port voltage (v) the solution of this pair of equations is obtained as the port current (i) of the circuit depicted in Fig. 6.
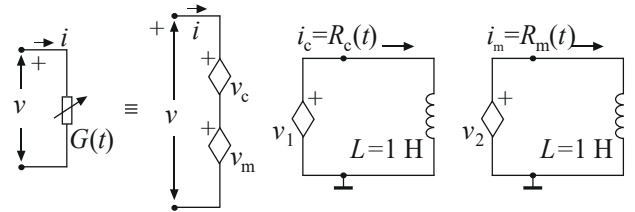

Figure 6. Circuit implementing the Habedank arc model

Here we have

$$(19a) \quad v_c=i \cdot R_c(t)$$

$$(19b) \quad v_m=i \cdot R_m(t)$$

$$(19c) \quad v_1 = \frac{dR_c(t)}{dt} = \frac{R_c(t)}{\tau_c}\left(1 - \frac{v^2(t)}{V_c^2}\frac{[R_c(t)+R_m(t)]^2}{R_m^2(t)}\right)$$

$$(19d) \quad v_2 = \frac{dR_m(t)}{dt} = \frac{R_m(t)}{\tau_m}\left(1 - \frac{v^2(t)}{P_0}\frac{[R_c(t)+R_m(t)]^2}{R_m(t) \cdot R_c^2(t)}\right)$$

The value of $G(t)$ corresponding to the reciprocal of the one expressed by (18), obtained by running the circuit of Fig. 4 by SPICE, is depicted in Fig. 5 denoted by 7. The following parameters were used for this simulation: $G_0=100$ S, $\tau_c=\tau_m=100$ ms, and $P_0=1000$ W, $V_c^2=1000$ V², $R_c(0)=R_m(0)=10$ mΩ.

2.6 The Schavemaker model

The Schavemaker model [14] is described by the following equation

$$(20) \quad \frac{1}{G(t)} \cdot \frac{dG(t)}{dt} = \frac{1}{\tau} \cdot \left(\frac{v(t) \cdot i(t)}{\max\left(V_{arc} \cdot |i|, P_0 + C \cdot v(t) \cdot i(t)\right)} - 1 \right).$$

This model is specific since it uses an approximating function with discontinuous derivative. From that point of view it is interesting and challenging for circuit implementation.

For implementation of this model one may use the circuit of Fig. 3 again with the following:

$$(21a) \quad i_1 = v \cdot v_2$$

$$(21c) \quad i_2 = -\frac{1}{\tau} \cdot v_2 + \frac{1}{\tau} \cdot v \cdot i \cdot \frac{1}{\max\left(V_{arc} \cdot \sqrt{i^2}, P_0 + C \cdot v \cdot i\right)}.$$

ON if $\left(V_{arc} \cdot \sqrt{i^2}\right) > \left(P_0 + C \cdot v \cdot i\right)$

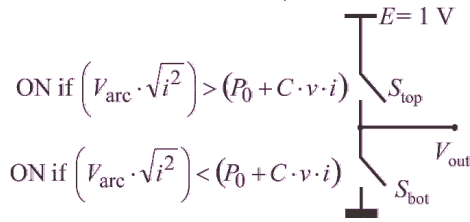ON if $\left(V_{arc} \cdot \sqrt{i^2}\right) < \left(P_0 + C \cdot v \cdot i\right)$

Figure 7. The comparator

To complete the circuit a comparator is needed producing an output voltage V_{out} such that

$$(22a) \quad V_{out}=1 \text{ if } \left(V_{arc} \cdot \sqrt{i^2}\right) > \left(P_0 + C \cdot v \cdot i\right),$$

$$(22b) \quad V_{out}=0, \text{ otherwise.}$$

Based to that the current i_3 was calculated as

$$(23) \quad i_3 = \frac{1}{V_{out} \cdot \left(V_{arc} \cdot \sqrt{i^2}\right) + \left(1 - V_{out}\right) \cdot \left(P_0 + C \cdot v \cdot i\right)}.$$

The comparator circuit used to create V_{out} of (22) is depicted in Fig. 7.

The value of $G(t)$ corresponding to the reciprocal of the one expressed by (18), obtained by running the circuit of Fig. 4 by SPICE, is depicted in Fig. 5 denoted by 3. The following parameters were used for this simulation: τ=10 ms, P_0=100 W; C_{int}=50 V_{arc}=1000 V G_0=100 S.

4. Conclusion

Implementation of the arc model equation in a form of electrical circuit is of crucial importance from the simulation point of view. Namely, when such circuit models are available, fault simulation is enabled for complex power systems including bus-bars, switchgears, power lines, cables, transformers etc. That in turn allows for successful design and maintenance of the grid.

Various models proposed in the literature were implemented here and simulated by the SPICE simulator. It is important, however, to have in mind here that the models described

may be used in any circuit simulator allowing for behavioural controlled sources to be used.

The simulation results show that by using different models different real-life situations may be captured and proper simulation to be performed. Having that in mind one is not in situation to give any recommendations or comparison of the model described as far.

6. References

[1] Hanson, J., and Koenig, D., "Fault Arcs Effects in Cable Bundles for Space Applications in Vacuum", IEEE Transactions on Dielectrics and Electrical Insulation, Vol. 4. No. 4, August 1997, pp. 394-399.

[2] Mishra, A.K., "Detection of Arcing in Low Voltage Distribution Systems", 2008 IEEE Region 10 Colloquium and the Third International Conference on Industrial and Information Systems, Kharagpur, INDIA December 8 -10, 2008. Paper ID 502.

[3] Ghezzi, L., and Balestrero, A., "Modeling and Simulation of Low Voltage Arcs", Technische Universiteit Delft, College voor Promoties, 2010.

4] Schavemaker, P. H., "Arc Model Blockset for use with MATLAB Simulink and Power System: Blockset-User's Guide," (Last visited October 14, 2015) http://www.ewi.tudelft.nl/fileadmin/Faculteit/EWI/Over _de_faculteit/Afdelingen/Electrical_Sustainable_Energ y/HCPS/EPS/downloads/doc/amb2.zip

[5] Yuan, L., Sun, L., "Simulation of Fault Arc Using Conventional Arc Models", Energy and Power Engineering, 2013, Vol. 5, pp. 833-837, doi:10.4236/ epe.2013.54B160.

[6] Kizilcay, M., and Pniok, T., "Digital Simulation of Fault Arcs in Powers systems", Europe Trans. Electr. Power Syst., ETEP, Vol. 4, pp. 55-59, 1991.

[7] Elkalashy, N. I., Lehtonen, M., Darwish, H. A., Izzularab, M. A., and Taalab, A.-M. I., "Modeling and Experimental Verification of High Impedance Arcing Fault in Medium Voltage Networks", IEEE Trans. on Dielectrics and Electrical Insulation, Vol. 14, No. 2, pp. 375-383, April 2007.

[8] Pikler, L., Kizilkay, M., Bán, G., and Handl, P., „Improved secondary arc models based on identification of arc parameters from staged fault test records", Proc. Of the 14th PSCC, Sevilla, June 2002, Session 24, Paper No. 3.

[9] Van Rensburg, K.J., „Analysis of Arcing Faults on Distribution Lines for Protection and Monitoring",

Master thesis, School of Electrical and Electronic Engineering, Quinsland University of Technology, 2003.

[10] Cassie, A. M., "Theorie Nouvelle des Arcs de Rupture et de la Rigidité des Circuits," CIGRE, Vol. 102, 1939, pp. 588-608.

[11] Schwarz, J., "Dynamisches Verhalten eines Gasbeblasenen, Turbulenzbestimmten Schaltlichtbogens," ETZ-A, Vol. 92, 1971, pp. 389-391.

[12] Mayr, O., "Beitrage zur Theorie des Statischen und des Dynamischen Lichtbogens," Archiv für Elektrotechnik, Vol. 37, No. 12, 1943, pp. 588-608.

[13] Mayr, O., "Über die Theorie des Lichtbogens und seiner Löschung," Elektrotechnische Zeitschrift, Vol. 64, No. 49-50, 1943, pp. 645-652.

[14] P. H. Schavemaker and L. Van der Sluis, "An Improved Mayr-Type Arc Model Based on Current-Zero Measurements," IEEE Transactions on Power Delivery, Vol. 15, No. 2, 2000, pp. 580-584. doi:10.1109/61.852988.

[15] Habedank, U., "On the Mathematical Description of Arc Behaviour in the Vicinity of Current Zero," etz Archiv, Vol. 10, No.11, 1988, pp. 339-343.